Modeling and identification of passenger car dynamics using robotics formalism

Gentiane Venture, Pierre-Jean Ripert, Wisama Khalil, Maxime Gautier, Philippe Bodson

Modelling and identification of passenger car dynamics using robotics formalism

Gentiane Venture (*IEEE member*), Pierre-Jean Ripert, Wisama Khalil (*IEEE Senior Member*), Maxime Gautier, Philippe Bodson

***Abstract*— This paper deals with the problem of dynamic modelling and identification of passenger cars. It presents a new method which is based on robotics techniques for modelling and description of tree structured multi-body systems. This method enables us to systematically obtain the dynamic identification model, which is linear with respect to the dynamic parameters. The estimation of the parameters is carried out using a weighted least squares method. The identification is tested using vehicle dynamics simulation software, used by the car manufacturer PSA Peugeot-Citroën, in order to define a set of trajectories with good excitation properties and to determine the number of degrees of freedom of the model. The method has then been used to estimate the dynamic parameters of an experimental Peugeot 406, which is equipped with different position, velocity and force sensors.**

***Index Terms*— Passenger car, modelling, identification, mobile robot dynamics.**

I. Introduction

CAR manufacturers have to design and build their cars faster than ever to meet the customers needs. Meanwhile, safety considerations are becoming more numerous and tests very strict. To fulfill these constraints, they have to make use of simulations and calculations as well as experiments. During the design of a car, simulation is used but not for the tuning of the prototype. In order to build tools that allow computing whilst tuning, it is necessary to have good knowledge of the prototype parameters for the different configurations of the car. Classical non-linear identification techniques to estimate the dynamic parameters are very difficult to apply on the car model due to the complexity of its state space model. For instance the authors of reference [1] use an output error method that is very time-consuming because of the integration of the direct dynamic model (state space model) at each step of the optimization algorithm. Besides, this technique is very sensitive to non linear optimization issues such as initial values and local minima. We suggest identifying the dynamic parameters using robotics techniques and tools, which are based on an identification model that is linear with respect to the dynamic parameters. This dynamic identification model is obtained using the inverse dynamic model that can be obtained systematically using a recursive Newton-Euler algorithm [2]. The proposed method is tested by simulation and on an experimental Peugeot 406. The simulation is carried out using the dynamic vehicle simulation software *ARHMM* [3]. The influence of the car trajectory, the number of degrees of freedom (*dof*) of the model, as well as the cut off frequency of filters, on the results of the estimation are studied.

II. Vehicle dynamics

Vehicle dynamics is the study of vehicle behavior whilst driving. Only some elements of the vehicle are needed to describe and model this behavior, they constitute the degrees of freedom (*dof*) of the car with respect to the ground and between the car components that link the chassis to ground [4]. The car is composed of:

- the chassis,
- the steering system,
- the four suspensions and the two anti-roll bars,
- the four unsprung bodies,
- the four wheels with their tires.

There are 8 *dof* for each wheel [5]:

- the track-width (Fig.1),
- the wheel-base (Fig.1),
- the suspension clearance,
- the toe angle of the rear wheel, the steering angle of the front wheel,
- the camber angle (Fig.1),
- the kingpin angle,
- the rotation of the wheel around its axis,
- the tire deflection.

Some of these *dof* are actuated, such as the steering angle or the rotation of the front wheels, but some others are elastic and elasto-kinematics deformations, such as suspension clearance. Car motion with respect to the ground is described by 6 degrees of freedom (Fig.2); 3 translational and 3 rotational, which are called:

- longitudinal translation,
- lateral translation,
- vertical translation,
- roll: rotation around the longitudinal axis,
- pitch: rotation around the transversal axis,
- yaw: rotation around the vertical axis.

The external forces applied to the car which have the most significant impact on vehicle dynamics, are the contact forces between the ground and the tires. These external forces are

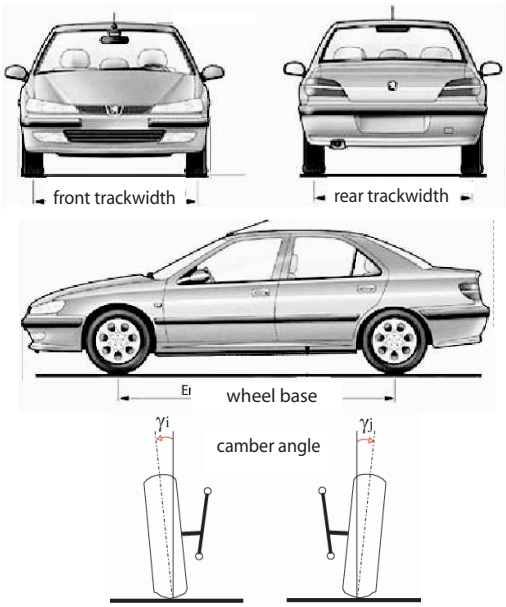

Fig. 1. Characteristic geometric parameters of the car dynamics

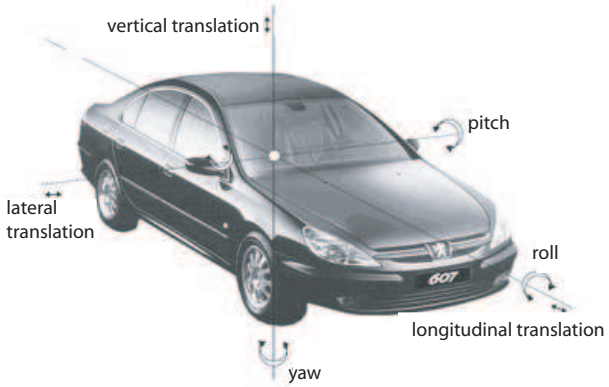

Fig. 2. Movements of the car body

difficult to model [6], [7], or to estimate [8], [9], but they can be measured at the center of the wheels using dynamometric wheels. Aerodynamic forces also have an effect on the vehicle behavior, particularly at high speed ($> 90km/h$) [4].

III. Computation of the car dynamics

A. Structure description and geometric modelling

To describe a passenger car we will use the modified Denavit and Hartenberg (MDH) notations [2], [10] that are commonly used in robotics. This description allows us to obtain, systematically, the identification dynamic model of the system, whatever the number of *dof*. The car is considered as a tree structured multi-body system, with n bodies, where the wheels represent the terminal links. Each body B_j is linked to its antecedent with a joint which represents an elementary *dof* either translational or rotational, the joint can be rigid or elastic. A body (or a link) can be real or virtual, the virtual bodies are introduced to describe joints with multiple *dof* or intermediate fixed frames. We define a reference frame R_i (O_i, $\boldsymbol{x}_i$, $\boldsymbol{y}_i$, $\boldsymbol{z}_i$) attached to each body B_i. The $\boldsymbol{z}_i$ axis is defined along the axis of joint i. An axis $\boldsymbol{u}_j$ is defined along the common normal between $\boldsymbol{z}_i$ and $\boldsymbol{z}_j$, where link i is the antecedent of link j, denoted by $i = a(j)$. The $\boldsymbol{x}_i$ axis is defined arbitrarily along one of the axes $\boldsymbol{u}_j$, with $a(j) = i$. The (4×4) homogenous transformation matrix ${}^i\boldsymbol{T}_j$ between two consecutive frames R_i and R_j is defined using the six following parameters [10] (Fig.3):

- γ_j: angle between $\boldsymbol{x}_i$ and $\boldsymbol{u}_j$ around the axis $\boldsymbol{z}_i$,
- b_j: distance between $\boldsymbol{x}_i$ and $\boldsymbol{u}_j$ along $\boldsymbol{z}_i$,
- α_j: angle between $\boldsymbol{z}_i$ and $\boldsymbol{z}_j$ around the axis $\boldsymbol{u}_j$,
- d_j: distance from $\boldsymbol{z}_i$ to $\boldsymbol{z}_j$ along $\boldsymbol{u}_j$,
- θ_j: angle between $\boldsymbol{u}_j$ and $\boldsymbol{x}_j$ around the axis $\boldsymbol{z}_j$,
- r_j: distance from $\boldsymbol{u}_j$ to $\boldsymbol{x}_j$ along $\boldsymbol{z}_j$.

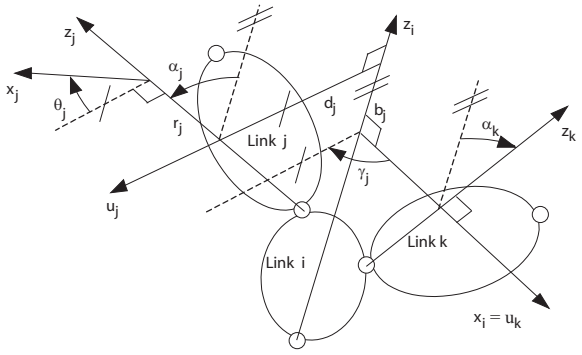

Fig. 3. The geometric parameters

In Fig.3, since $\boldsymbol{x}_i$ is taken along $\boldsymbol{u}_k$, the parameters γ_k and b_k are equal to zero. The transformation matrix between frames i and j is represented by the following (4×4) matrix:

$$ {}^i\boldsymbol{T}_j = \begin{bmatrix} {}^i\boldsymbol{A}_j & {}^i\boldsymbol{P}_j \\ \boldsymbol{0}_{3\times1} & 0 \end{bmatrix} \tag{1} $$

where:

- ${}^i\boldsymbol{A}_j$ is the (3×3) rotation matrix of frame j with respect to frame i,
- ${}^i\boldsymbol{P}_j$ is the (3×1) vector defining the origin of frame j with respect to frame i.

The generalized coordinate of joint j is denoted q_j, it is equal to r_j if j is translational and θ_j if j is rotational. We define the parameter $\sigma_j = 1$ if joint j is translational, and $\sigma_j = 0$ if joint j is rotational, $\overline{\sigma_j} = 1 - \sigma_j$. If there is no *dof* between two frames that are fixed with respect to each other, we take $\sigma_j = 2$. This means that the time derivative of q_j is zero.

B. Dynamic modelling

1) Dynamic parameters: a set of 10 inertial parameters is associated with each real body B_j. It consists of:

- the mass M_j,
- the 6 independent components of the inertia matrix $\boldsymbol{J}_j$ given in frame R_j, denoted by XX_j, XY_j, XZ_j, YY_j, YZ_j, ZZ_j,
- the components MX_j, MY_j, MZ_j of the first moments vectors $\boldsymbol{MS}_j$ with respect to frame R_j.

When joint j is elastic, we define the following parameters:

- the stiffness k_j of the joint,
- the damping coefficient h_j,
- the Coulomb coefficient f_{sj}.

The vector of standard dynamic parameters of the system, which is denoted $\boldsymbol{X}_S$, is composed of the previous parameters for all the links.

2) The Lagrange dynamic model of the car: the Lagrange formalism expresses the movement of each body in terms of the joint coordinates $\boldsymbol{q} = [q_1, \ldots, q_n]$, its first and second derivatives $\dot{\boldsymbol{q}}$, $\ddot{\boldsymbol{q}}$, the external moments and forces applied on the system $\boldsymbol{F}_e$ and the vector of dynamic parameters $\boldsymbol{X}_S$. It is expressed as:

$$\boldsymbol{f}\left(\boldsymbol{q}, \dot{\boldsymbol{q}}, \ddot{\boldsymbol{q}}, \boldsymbol{F}_e, \boldsymbol{X}_S\right) = \boldsymbol{0} \tag{2}$$

To use the Lagrange method, the movement of the car body with respect to ground is defined with a 6 *dof* chain, the first 3 are translational and the last 3 are rotational [11], [12]. This chain is represented by 5 virtual bodies (B_1 to B_5) with zero inertial parameters, the 6^{th} body B_6 is the chassis. The reference body B_0 is the ground. In this case the inverse dynamic model, giving the joint torques, is obtained with the following general equation:

$$\boldsymbol{\Gamma} + \boldsymbol{Q} = \boldsymbol{\Gamma}^e + \boldsymbol{\Gamma}^f + \boldsymbol{H}\left(\boldsymbol{q}, \dot{\boldsymbol{q}}, \ddot{\boldsymbol{q}}, \boldsymbol{X}_S\right) \tag{3}$$

where:

- $\boldsymbol{\Gamma}$ is the vector of joint forces or torques
- $\boldsymbol{Q}$ is the vector of generalized efforts representing the projection of the external forces and torques on the joint axes, it is calculated with:

$$\boldsymbol{Q} = -\sum \boldsymbol{G}_j(\boldsymbol{q})^T \boldsymbol{F}_{ej} \tag{4}$$

- $\boldsymbol{G}_j(\boldsymbol{q})$ is the Jacobian matrix of frame R_j
- $\boldsymbol{F}_{ej}$ is the vector of external forces $\boldsymbol{f}_{ej}$ and moments $\boldsymbol{m}_{ej}$ applied by body B_j on the environment,
- $\boldsymbol{H}$ is the vector of inertial, Coriolis, centrifugal and gravity forces,
- $\boldsymbol{\Gamma}^e$ is the joint elastic force. The j^{th} element of $\boldsymbol{\Gamma}_e$ is written as:
  - if j is an elastic joint:

$$\Gamma_j^e = k_j q_j + off_j \tag{5}$$

with q_j the joint co-ordinate j with respect to the original position and k_j the stiffness of joint j, off_j an offset,

  - if j is not an elastic joint $\Gamma_j^e = 0$
- $\boldsymbol{\Gamma}^f$ is the friction force. Friction is modelled using a viscous parameter h_j and a Coulomb parameter f_{sj}:

$$\Gamma_j^f = h_j \dot{q}_j + f_{Sj} sign(\dot{q}_j) \tag{6}$$

In the following we note: $\boldsymbol{L} = \boldsymbol{\Gamma} + \boldsymbol{Q}$.

3) Practical calculation of the Lagrange dynamic model: the Lagrange model is typically calculated using the Lagrange equation, which calculates the kinetic and potential energies of all the elements of the mechanical system. The generalized forces $\boldsymbol{Q}$ are calculated using (4) or by applying the virtual work principle [4], [7]. The Lagrange model can be calculated more easily using a recursive algorithm based on the Newton-Euler equation, after expressing the link velocities and accelerations in terms of joint positions, velocities and accelerations [10], [13]. This algorithm consists of two recursive calculations. The forward one calculates the total forces and moments on each body, while the backward one leads to calculation of the joint torques.

The forward recursive calculation can be summarized as follows: for $j = 1$ to n, we calculate successively:

$${}^j\boldsymbol{\omega}_i = {}^j\boldsymbol{A}_i \, {}^i\boldsymbol{\omega}_i \tag{7}$$

$${}^j\boldsymbol{\omega}_j = {}^j\boldsymbol{\omega}_i + \bar{\sigma}_j \dot{q}_j \, {}^j\boldsymbol{a}_j \tag{8}$$

$${}^j\dot{\boldsymbol{\omega}}_j = {}^j\boldsymbol{A}_i \, {}^i\dot{\boldsymbol{\omega}}_i + \bar{\sigma}_j \left(\ddot{q}_j \, {}^j\boldsymbol{a}_j + {}^j\boldsymbol{\omega}_i \times \dot{q}_j \, {}^j\boldsymbol{a}_j\right) \tag{9}$$

$$\begin{aligned} {}^j\dot{\boldsymbol{V}}_j = {}^j\boldsymbol{A}_i \left[{}^i\dot{\boldsymbol{V}}_i + \left({}^i\widetilde{\dot{\boldsymbol{\omega}}}_i + {}^i\widetilde{\boldsymbol{\omega}}_i \, {}^i\widetilde{\boldsymbol{\omega}}_i\right) {}^i\boldsymbol{P}_j\right] \\ + \sigma_j \left(\ddot{q}_j \, {}^j\boldsymbol{a}_j + 2 \, {}^j\boldsymbol{\omega}_i \times \dot{q}_j \, {}^j\boldsymbol{a}_j\right) \end{aligned} \tag{10}$$

$${}^j\boldsymbol{F}_j = M_j \, {}^j\dot{\boldsymbol{V}}_j + \left({}^j\widetilde{\dot{\boldsymbol{\omega}}}_j + {}^j\widetilde{\boldsymbol{\omega}}_j \, {}^j\widetilde{\boldsymbol{\omega}}_j\right) {}^j\boldsymbol{MS}_j \tag{11}$$

$${}^j\boldsymbol{M}_j = {}^j\boldsymbol{J}_j \, {}^j\dot{\boldsymbol{\omega}}_j + {}^j\boldsymbol{\omega}_j \times \left({}^j\boldsymbol{J}_j \, {}^j\boldsymbol{\omega}_j\right) + {}^j\boldsymbol{MS}_j \times {}^j\dot{\boldsymbol{V}}_j \tag{12}$$

with the upper left exponent denoting the projection frame, $\times$ denoting the outer vector product and:

- $i = a(j)$
- $\dot{\boldsymbol{\omega}}_j$ is the angular acceleration of body j,
- $\boldsymbol{\omega}_j$ is the angular velocity of body j,
- $\widetilde{\boldsymbol{\omega}}$ is the skew-symmetric matrix associated to the vector product, defined from the components of the (3×1) vector by:

$$\widetilde{\boldsymbol{\omega}} = \begin{bmatrix} 0 & -\omega_z & \omega_y \\ \omega_z & 0 & -\omega_x \\ -\omega_y & \omega_x & 0 \end{bmatrix} \tag{13}$$

- $\dot{\boldsymbol{V}}_j$ acceleration of O_j, origin of frame j,
- $\boldsymbol{F}_j$ total forces applied on body j

- $\boldsymbol{M}_j$ total moments applied on body j with respect to O_j,
- ${}^j\boldsymbol{A}_i$ the (3×3) orientation matrix of frame R_i in R_j,
- $\boldsymbol{a}_j$ is the unit vector along $\boldsymbol{z}_j$, thus ${}^j\boldsymbol{a}_j = [0\ 0\ 1]^T$,
- M_j, $\boldsymbol{MS}_j$ and $\boldsymbol{J}_j$ defined in section III.B.1.

The forward calculation is initialized with ${}^0\boldsymbol{\omega}_0 = \boldsymbol{0}$, ${}^0\dot{\boldsymbol{\omega}}_0 = \boldsymbol{0}$, whereas the translational acceleration of frame 0 will be set equal to gravity $\boldsymbol{g}$ with opposite sign, thus ${}^0\dot{\boldsymbol{V}}_0 = -\boldsymbol{g}$, in order to automatically take into account the effect of the gravity forces.

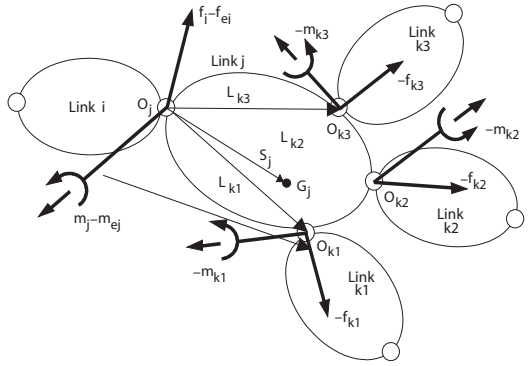

Fig. 4. Forces and moments acting on a link of a tree structure

The backward recursive equations, for $j = n, \ldots, 1$ calculate the forces ${}^j\boldsymbol{f}_j$ and moments ${}^j\boldsymbol{m}_j$ exerted on body B_j by its antecedent body B_i (Fig.4), they are:

$$ {}^j\boldsymbol{f}_j = {}^j\boldsymbol{F}_j + {}^j\boldsymbol{f}_{ej} + \sum_{s(j)} {}^j\boldsymbol{f}_{s(j)} \tag{14} $$

$$ {}^i\boldsymbol{f}_j = {}^i\boldsymbol{A}_j\, {}^j\boldsymbol{f}_j \tag{15} $$

$$ {}^j\boldsymbol{m}_j = {}^j\boldsymbol{M}_j + {}^j\boldsymbol{m}_{ej} + \sum_{s(j)} {}^j\boldsymbol{A}_{s(j)}\, {}^{s(j)}\boldsymbol{m}_{s(j)} + {}^j\widetilde{\boldsymbol{P}}_{s(j)}\, {}^j\boldsymbol{f}_{s(j)} \tag{16} $$

with:

- $s(j)$ indicating the bodies whose antecedent is body B_j
- ${}^j\boldsymbol{f}_{ej}$, ${}^j\boldsymbol{m}_{ej}$ the external forces and moments applied by body B_j on the environment

The joint forces (or torques) are obtained by projecting ${}^i\boldsymbol{f}_j$ (or ${}^i\boldsymbol{m}_j$) on the joint axis $\boldsymbol{z}_j$ and by taking into account the effects of friction and elasticity as follows:

$$ \Gamma_j = \left(\sigma_j\, {}^j\boldsymbol{f}_j + \bar{\sigma}_j\, {}^j\boldsymbol{m}_j\right)^T\, {}^j\boldsymbol{a}_j + \Gamma_j^f + \Gamma_j^e \tag{17} $$

This backward calculation is initialized by putting ${}^j\boldsymbol{f}_j$, ${}^j\boldsymbol{m}_j$ equal to zero for the terminal links. We can note that the contact forces between the tire and the road will be taken into account through $\boldsymbol{f}_{ej}$ and $\boldsymbol{m}_{ej}$ of the terminal links (the wheels). The projection of these forces on the joint axes will be obtained systematically without application of equation (4) as would be the case if the Lagrange equation was used. It is to be noted that this algorithm can be programmed numerically or symbolically. To optimize the number of its operations, we use customized symbolic techniques to implement it [10]. It can be proven that the dynamic model is linear with respect to the standard dynamic parameters, thus (3) can be rewritten as:

$$ \boldsymbol{L} = \boldsymbol{D}_S\left(\boldsymbol{q}, \dot{\boldsymbol{q}}, \ddot{\boldsymbol{q}}\right) \boldsymbol{X}_S \tag{18} $$

where matrix $\boldsymbol{D}_S$ is a function of $(\boldsymbol{q}, \dot{\boldsymbol{q}}, \ddot{\boldsymbol{q}})$.
The inertial parameters of the chassis appear explicitly in the first six equations giving L_1 to L_6.

4) Mixed Newton-Lagrange model: the Newton-Euler formalism expresses the movement of a body in terms of its rotational speed, rotational acceleration, translational acceleration and its current position $[\boldsymbol{\omega}, \dot{\boldsymbol{\omega}}, \dot{\boldsymbol{V}}, \boldsymbol{\Phi}]$.
We will suggest another form of the dynamic model that combines both Newton-Euler and Lagrange approaches, in order to obtain a more efficient model of the car. In this case the body of the car is represented by one body denoted by B_1, whose dynamic equations are expressed in terms of the Euler variables $[\dot{\boldsymbol{V}}_1, \boldsymbol{\omega}_1, \dot{\boldsymbol{\omega}}_1]$, while the rest of the system dynamics (Bodies B_2 to B_n) is expressed in terms of Lagrange variables $(\boldsymbol{q}, \dot{\boldsymbol{q}}, \ddot{\boldsymbol{q}})$. The main advantages of this method is that the Euler variables of the chassis correspond to the measured variables in an experimental system and that the transformation matrices between the first 6 frames of the Lagrange model no longer exist. This enables us to obtain a more compact dynamic model and to reduce the number of mathematical operations required. The dynamic equations of this mixed model can be obtained by the recursive algorithm presented in section III.B.3 with the following modifications:

- The value of n is reduced by 5,
- In the forward recursive calculations, for $j = 1$, the total forces and moments on the chassis $\boldsymbol{F}_1$ and $\boldsymbol{M}_1$ are calculated using (11) and (12) as a function of $[\dot{\boldsymbol{V}}_1, \boldsymbol{\omega}_1, \dot{\boldsymbol{\omega}}_1]$. For this first iteration, the other equations are not required.
- The equations of the chassis will be represented by the total forces and moments ${}^1\boldsymbol{f}_1$ and ${}^1\boldsymbol{m}_1$ exerted by link 0 on link 1, using equations (14) to (16), we note that (17) has no use in this case. Thus the first 6 equations of the Lagrange model (L_1,...,L_6) will be replaced by the following 6 equations:

$$ [\boldsymbol{0}_{6\times 1}] = \begin{bmatrix} {}^1\boldsymbol{f}_1 \\ {}^1\boldsymbol{m}_1 \end{bmatrix} \tag{19} $$

  ${}^1\boldsymbol{f}_1$ and ${}^1\boldsymbol{m}_1$ are zero because there is no body antecedent to the chassis. The complete model can be expressed as a linear relation in the dynamic parameters:

$$ \boldsymbol{L} = \boldsymbol{D}_S\left(\boldsymbol{\omega}_1, \dot{\boldsymbol{\omega}}_1, \dot{\boldsymbol{V}}_1, \boldsymbol{q}, \dot{\boldsymbol{q}}, \ddot{\boldsymbol{q}}\right) \boldsymbol{X}_S \tag{20} $$

5) Base dynamic parameters: the base dynamic parameters are the minimum number of parameters that can be used to compute the dynamic model and they constitute

the identifiable parameters that can be estimated using an identification method based on the dynamic model [10]. The base parameters are obtained from the standard dynamic parameters by grouping some parameters together and by eliminating those that have no effect on the dynamic model. Two methods are available for the computation of the base parameters: a symbolical method [14] or a numerical method based on the *QR* decomposition [15]. The numerical method allows considering the grouping relations due to the poor excitation properties of the chosen identification trajectory. After determining the identifiable parameters, the Lagrange dynamic identification model (18) becomes:

$$\boldsymbol{L} = \boldsymbol{D}\left(\boldsymbol{q}, \dot{\boldsymbol{q}}, \ddot{\boldsymbol{q}}\right) \boldsymbol{X} \tag{21}$$

where:

- $\boldsymbol{X}$ is the vector of n_B base parameters
- $\boldsymbol{D}$ is the $(n \times n_B)$ matrix deduced from $\boldsymbol{D}_S$ by only taking into account the columns corresponding to the base parameters

A similar relation for the mixed Newton-Lagrange model can be deduced from (20).

IV. Identification method

We suggest making use of the fact that the dynamic model is linear in the dynamic parameters to identify the base parameters using linear least square optimization techniques [10], [16].

A. Identification model sampling

The dynamic model (21) is sampled along a trajectory. All the n_e samples for the n equations are collected in a linear system of equations as follows:

$$\boldsymbol{Y} = \boldsymbol{W}\left(\boldsymbol{q}, \dot{\boldsymbol{q}}, \ddot{\boldsymbol{q}}\right) \boldsymbol{X} + \boldsymbol{\rho} \tag{22}$$

where:

- $\boldsymbol{Y}$ is the $((n \times n_e) \times 1)$ vector of joint torques, obtained by sampling $\boldsymbol{L}$, sorted by joint:

$$\boldsymbol{Y} = \begin{bmatrix} \boldsymbol{Y}_1 \\ \vdots \\ \boldsymbol{Y}_n \end{bmatrix}$$

- $\boldsymbol{Y}_j$ the $(n_e \times 1)$ vector of joint forces, or torques associated to joint j
- $\boldsymbol{W}$ is the $((n \times n_e) \times n_B)$ observation matrix, obtained by sampling $\boldsymbol{D}$ and sorted by joint:

$$\boldsymbol{W} = \begin{bmatrix} \boldsymbol{W}_1 \\ \vdots \\ \boldsymbol{W}_n \end{bmatrix}$$

- $\boldsymbol{W}_j$ the $(n_e \times n_B)$ observation matrix associated with joint j,
- $\boldsymbol{\rho}$ the $((n \times n_e) \times 1)$ vector of modelling errors.

B. Resolution and interpretation of results

Equation (22) can be solved using the weighted least squares (WLS) which is implemented in many software packages with efficient algorithms (Matlab, Scilab). Because the equations are sorted by joint, the linear system is composed of n subsystems each with n_e equations. The weighting procedure is defined in order to ensure the most significant equations [16], [17]. The weighted matrix $\boldsymbol{P}$ is computed using an estimation of the standard deviation for each joint subsystem j, $\sigma_{\rho j}$, as follows:

$$\boldsymbol{P} = \begin{bmatrix} \boldsymbol{S}_1 & & \\ & \ddots & \\ & & \boldsymbol{S}_n \end{bmatrix} \tag{23}$$

with:

- $\boldsymbol{S}_j = \boldsymbol{I}_{n_e}/\sigma_{\rho j}$,
- $\boldsymbol{I}_{n_e}$ the $(n_e \times n_e)$ identity matrix,
- $\sigma_{\rho j}$ is calculated by:

$$\sigma_{\rho j}^2 = \frac{\| \boldsymbol{Y}_j - \boldsymbol{W}_j \hat{\boldsymbol{X}}^j \|^2}{n_e - n_{Bj}} \tag{24}$$

- n_{Bj} the number of base parameters appearing in the equations of joint j,
- $\hat{\boldsymbol{X}}^j$ the $(n_{Bj} \times 1)$ vector of estimated parameters using joint j equations,

The weighted system to be solved is then given by:

$$\boldsymbol{Y}_P = \boldsymbol{W}_P \boldsymbol{X} + \boldsymbol{\rho}_P \tag{25}$$

where $\boldsymbol{Y}_P = \boldsymbol{P}\boldsymbol{Y}$, $\boldsymbol{W}_P = \boldsymbol{P}\boldsymbol{W}$ and $\boldsymbol{\rho}_P = \boldsymbol{P}\boldsymbol{\rho}$.

Standard deviations on the estimated values $\sigma_{\hat{X}j}$ are computed using classical and simple results from statistics, considering the matrix $\boldsymbol{W}$ to be a deterministic one, and $\boldsymbol{\rho}$ to be a zero mean additive independent noise, with standard deviation such that:

$$\boldsymbol{C}_{\rho\rho} = E(\rho^T \rho) = \sigma_\rho^2 \boldsymbol{I}_{n_e \times n}$$

where E is the expectation operator.
An unbiased estimation of σ_ρ is used:

$$\sigma_\rho^2 = \frac{\| \boldsymbol{Y}_P - \boldsymbol{W}_P \hat{\boldsymbol{X}} \|^2}{n \times n_e - n_B} \tag{26}$$

The covariance matrix of the estimation error and standard deviations can be calculated by:

$$\boldsymbol{C}_{\hat{X}\hat{X}} = E\left((\boldsymbol{X} - \hat{\boldsymbol{X}})(\boldsymbol{X} - \hat{\boldsymbol{X}})^T\right) = \sigma_p^2 (\boldsymbol{W}_P^T \boldsymbol{W}_P)^{-1} \tag{27}$$

$\sigma_{\hat{X}j} = \sqrt{\boldsymbol{C}_{\hat{X}\hat{X}}(j,j)}$ is the i^{th} diagonal coefficient of $\boldsymbol{C}_{\hat{X}\hat{X}}$. The relative standard deviation $\sigma_{\hat{X}j\%}$ is given by:

$$\sigma_{\hat{X}j\%} = 100 \frac{\sigma_{\hat{X}j}}{| \hat{X}_j |} \tag{28}$$

Assuming that $\sigma_{\hat{X}j}$ is the realization of a Gaussian random variable, the 95% confidence interval is $2\sigma_{\hat{X}j}$ and the relative

confidence interval is $2\sigma_{\hat{X}j\%}$. Then we consider that a parameter with a relative confidence interval lower than 10% is well identified, keeping in mind that this is only an indicator based on statistical assumptions. The parameters which are not well identified may be not excited by the identification trajectory, or may have only a small effect on the dynamic model, so they can be removed from the model [18]. But it is to be noted that this criterion is not a deterministic one in particular for parameters with small values, where they may be well identified although $\sigma_{\hat{X}j\%}$ is more than 10.

C. Filtering

Some joint variables must be estimated by the differentiation or the integration of the measurements. Derivatives are estimated with digital zero-phase pass band filters calculated as the product of a low pass Butterworth filter and a central derivative algorithm (29). The Butterworth filter is implemented as a Matlab function *filtfilt* which is a zero-phase forward and reverse digital filtering. Integrations are zero-phase estimated as the product of a high pass Butterworth filter and a trapezoidal algorithm (30).

$$f_d(t_k) = \frac{f(t_{k+1}) - f(t_{k-1})}{2T_e} \tag{29}$$

$$f_i(t_k) = f_i(t_{k-1}) + \frac{T_e}{2}\left(f(t_k) + f(t_{k-1})\right) \tag{30}$$

where f_d denotes the derivative, f_i denotes the integral and T_e denotes the sampling period.

D. Choosing a trajectory with sufficient excitation

The result of the estimation highly depends on the trajectory chosen for the identification [19], [20]. The excitation criteria are based on the calculation of a function of the condition number of the observation matrix $\boldsymbol{W}$ of the linear system [18]. Trajectories with sufficient excitation are defined using the simulation software *ARHMM* [3]. It has been shown that one kind of trajectory is enough to estimate the main dynamic parameters of a car: the "sinusoidal steering" at different speeds: $90km/h$ to $160km/h$.

V. Experimental car

A. Available sensors

Experiments are carried out on a Peugeot 406 car equipped with the following sensors:

- 1 SAGEM inertial unit giving the chassis angular velocities and translational accelerations with respect to the ground (*cof* (cut-off frequency): $10\,Hz$),
- 4 position sensors giving the clearance of the 4 suspension (*cof*: $20\,Hz$),
- 1 Correvit speed sensor giving lateral and longitudinal velocities of the chassis (*cof*: $15\,Hz$),
- 4 Zimmer laser sensors giving the 4 steering angles (*cof*: $10\,Hz$),
- 4 Eagle dynamometric wheels giving the 4 effort torques applied to the 4 wheel centers and the wheel angular position (*cof*: $100\,Hz$),
- 4 Zimmer laser sensors giving the vertical position of 4 points of the chassis with respect to the ground (*cof*: $20\,Hz$)

B. Computation of the missing data

Some joint variables required in the computation of the dynamic model cannot be measured by given sensors (particularly half track width, wheelbase and kingpin variations). To access these variables, car manufacturers work with tabulation models. These are characterized on test benches and return geometric and elasto-kinematics deformations of the axle systems as a function of the suspension clearance and the position of the steering wheel. Half track width, wheelbase and kingpin variations can be obtained in this way. The aerodynamic forces can be also obtained from tables as a function of the vehicle speed or must be identified (see section V.D).

C. Geometric modelling

The first modelling approach of the car dynamics is to consider the 6 *dof* between the ground and the chassis and all the *dof* between the chassis and the wheels. The corresponding system has 38 *dof*. The model is calculated usimg a mixed Newton-Lagrange as presented in section III.B.4. The chassis dynamics is calculated using the Euler variables while the branches are modelled using the Lagrange variables. This approach is more convenient with regard to the sensors available with our car and particularly with the use of an inertial unit. This model limits the projections of the measured variables on the car axes, thus measurement noises are minimized. Moreover, there are about 30% less mathematical operations (additions and multiplications) than with the Lagrange model.
For the left rear branch (Fig.5) the *dof* are:

- the half track width l_3,
- the wheelbase L,
- the suspension clearance z_3 (elastic joint),
- the toe angle β_3,
- the camber angle γ_3,
- the kingpin angle ζ_3,
- the angular position of the wheel θ_9,
- the vertical tire deflection z_{t3} (elastic joint).

The geometric parameters of the left rear branch (branch 3) are presented in Table I. The chassis constitutes the first link, its fixed frame R_1 is denoted R_c. The fixed frame R_8 is used to define the dynamometer measuring frame.

TABLE I

GEOMETRIC PARAMETERS OF THE LEFT REAR BRANCH (BRANCH 3) OF THE 38 *dof* MODEL

j	$a(j)$	σ_j	γ_j	b_j	α_j	d_j	θ_j	r_j
1	0	2	0	0	0	0	0	0
2	1	1	0	0	$-\pi/2$	0	$-\pi/2$	l_3
3	2	1	0	0	$-\pi/2$	0	$-\pi/2$	L
4	3	1	0	0	$-\pi/2$	0	0	z_3
5	4	0	0	0	0	0	β_3	0
6	5	0	0	0	$\pi/2$	0	$\pi/2+\gamma_3$	0
7	6	0	0	0	$\pi/2$	0	$\pi/2+\zeta_3$	0
8	7	2	0	0	$\pi/2$	0	0	0
9	8	0	0	0	$-\pi/2$	0	θ_9	0
10	8	1	0	0	0	0	0	z_{t3}

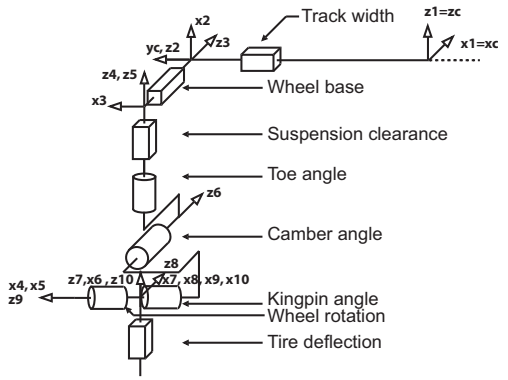

Fig. 5. Geometric modelling of the left rear branch (branch 3)

The vertical tire deflection is represented by an elastic prismatic joint. The right rear branch (branch 4) is similar to the left rear branch but with $j = 11$ to 19. For the front, there is the same number of *dof* where the toe angle β_j is replaced by the steering angle, thus $j = 20$ to 28 for the left front branch (branch 1) and $j = 29$ to 37 for the right front branch (branch 2).

D. Dynamic identification model

The dynamic identification model (20) is obtained using the symbolic software package *SYMORO+* [21], in which the algorithms given in section III.B are implemented. Knowing the geometric parameters, this software automatically gives the identification model which is linear in the dynamic parameters.

Since the contact forces are measured at the center of the wheel by the dynamometric wheels, the inertial parameters of the wheels are not identified. Only chassis and unsprung body inertial parameters represent the inertial parameters to be identified. All the other bodies are virtual and their inertial parameters are equal to 0. The suspension parameters to be estimated are composed of stiffness and friction parameters and an offset as defined in (5) and (6). Anti-roll bars are added at the front and rear to introduce a coupling between right and left suspension clearances. They are modelled by:

$$F_{ari} = k_{ar}(q_i - q_{opi}) \tag{31}$$

with:

- F_{ari} the force due to the anti-roll bar on suspension i,
- k_{ar} the anti-roll bar stiffness, in N/m,
- q_i the suspensions' clearance of the considered branch, in m,
- q_{opi} the suspensions' clearance of the opposite branch, in m.

Thus 2 more parameters are needed: k_{arr} for the rear bar and k_{arf} for the front bar.

The aerodynamic forces and moments, which are applied to the chassis, are denoted by:

$$
{}^c\tau_a = \begin{Bmatrix} F_{x_a} & C_{x_a} \\ F_{y_a} & C_{y_a} \\ F_{z_a} & C_{z_a} \end{Bmatrix}
$$

$$
= \begin{Bmatrix} \frac{1}{2}\rho_{air} S_z V_a^2 & \frac{1}{2}\rho_{air} L S_n V_a^2 \\ -\frac{1}{2}\rho_{air} S_y V_a^2 & -\frac{1}{2}\rho_{air} L S_m V_a^2 + z_C \frac{1}{2}\rho_{air} S_x V_a^2 \\ -\frac{1}{2}\rho_{air} S_x V_a^2 & -\frac{1}{2}\rho_{air} L S_l V_a^2 + z_C \frac{1}{2}\rho_{air} S_y V_a^2 \end{Bmatrix}
$$

with:

- ${}^c\tau_a$ the aerodynamic forces and torques given in the frame fixed to the chassis R_c, whose $\boldsymbol{x}_c$, $\boldsymbol{y}_c$ and $\boldsymbol{z}_c$ axes are along the longitudinal, lateral and vertical axes (Fig.2) of the chassis respectively,
- ρ_{air} the density of the air,
- L the wheel-base,
- z_C the vertical position of the origin of the frame R_c with respect to the front axle,
- S_x, S_y, S_z the drag coefficients of the vehicle in the air along the longitudinal direction, the transversal direction, and the vertical direction,
- S_l, S_m, S_n the drag coefficients of the vehicle in the air around the longitudinal direction, the transversal direction, and the vertical direction,
- V_a the norm of the vector $\boldsymbol{V}_a$ of aerodynamic velocity computed as follows: $\boldsymbol{V}_a = \boldsymbol{V}_{air} - \boldsymbol{V}_1$,
- $\boldsymbol{V}_{air}$ the speed of the air given in R_c. Because it is not measured it is supposed to be null,
- $\boldsymbol{V}_1$ the speed of the vehicle given in R_c.

These forces are identified via the model:

$$
{}^c\tau_a = \begin{Bmatrix} C_x V_a^2 & C_l V_a^2 \\ C_y V_a^2 & C_m V_a^2 \\ C_z V_a^2 & C_n V_a^2 \end{Bmatrix} \tag{32}
$$

where the C_i parameters are added to the parameters to be identified.

VI. SIMULATION OF THE CAR IDENTIFICATION

The car model is composed of 38 *dof* and 5 physical inertial bodies with 10 inertial parameters for each. Furthermore, each

of the suspensions needs 4 parameters, each of the anti roll-bars and aerodynamic forces or torques also need one parameter. Thus, this model is quite complex and certainly needs to be simplified in order to be correlated with the accuracy of the measurements and the available trajectories. This section presents a study of the robustness of the dynamic model generated in the previous step with respect to trajectories and perturbations. The software package ARHMM [3] is used to generate trajectories without perturbation using a set of known parameters. This software uses a dynamic algorithm representing the maximum phenomena existing in a real car so that it can describe the whole range of uses of the car and it is run with a real time core. It takes into account the driver's inputs through the transfer line and the steering wheel, as well as elastokinematic deformations, aerodynamics and non-linearity of the suspensions and anti-roll bars. Contact forces with the ground are given by the Pacejka's Magic Formula [6] and [7]. It gives a more precise model of a real car than the 38 *dof* model. The trajectory available is sinusoidal steering at different speeds. At first, the model with 38 *dof* is used to determine whether all the standard parameters are excited. Then, the model is modified consequently by deleting or grouping together some parameters.

A. Aerodynamic effect

With the sinusoidal steering trajectory, it appears that aerodynamic contribution is constant. Indeed, it is proportional to the vehicle speed which is constant in the tests used. Aerodynamic forces are therefore estimated from tabulations. Only the coefficient C_x of the aerodynamic force along the $\boldsymbol{x}$ axis is identified, because it is the most important component. The value of the other coefficients are too small to be identified.

B. Robust practical model

The following conclusions and simplifications have been deduced through different simulations using ARMMH and analyzing experimental data and results:

- The results are sensitive to measurement cut-off frequencies: to explain this sensitivity, a fast Fourier transform is applied to the measurements to determine the modes of each one. It appears that:
  - the data from the inertial unit are perturbed by the driveline (modes at 3.9 - 4.3 - 5.5 Hz),
  - camber and steering angle measurements are perturbed by the driveline (modes at 3.9 - 4.3 - 5.5 Hz),
  - only suspension clearances have "rebound of the wheel" mode information (mode at 12.7 Hz)

  To remove driveline perturbation, all the measurements are filtered with a low pass filter having a cut-off frequency of 3.125 Hz except suspension clearance which is not filtered to preserve the "rebound of the wheel" mode. The 3.125 Hz value is chosen because it preserves mechanical modes of the chassis which are between 0.4 and 3 Hz.
- Most of the unsprung body inertial parameters are not excited. Only their masses are to be considered, the other 9 inertial parameters are removed from the identification.
- Moreover track-width, wheel base, steering, camber or kingpin have negligible influence in dynamic identification and can be removed from the model. This will be shown by applying the experimental tests to the complete model of 38 *dof* and a reduced model of 20 *dof*.
- The dynamic equations to be used for the identification are restricted to the 6 components of the chassis and the 4 related to suspension clearances.

VII. Practical identification results

The identification method has been applied to an experimental Peugeot 406 car. Only sinusoidal steering trajectories are available. The 38 *dof* and the reduced 20 *dof* model are tested. The a priori parameters of the car, provided by Peugeot-Citroën are shown in Table II. They do not take into account the driver nor the equipment so they give only an idea about their values. It is to be noted that no a priori values are provided by the manufacturer for the Coulomb parameters.

A. Identification with a 38 dof model

Results of the identification on the model having 38 *dof* are given in Table II. As pointed out in section IV.B, the identification relative standard deviation $\sigma_{\hat{X}j\%}$ is used to give the following interpretation to the results: If $\sigma_{\hat{X}j\%} < 10\%$, the parameter is considered as well identified. Nevertheless this interpretation is not an absolute criterion; it could be even wrong if the parameter value is low. Applied to the obtained results the following parameters are considered as being well identified and the identification values are close to the a priori values: M_c, MX_c, XX_c, YY_c, ZZ_c, XZ_c, M_1, M_2, M_3, M_4, k_{arr}, k_{arf}, k_1, h_1, off_1, k_2, f_{s2}, h_2, off_2, k_3, h_3, off_3, k_4, h_4, off_4, C_x. Whereas the following parameters appear not to be well identified: MY_c, MZ_c, XY_c, YZ_c, f_{s1}, f_{s3}, f_{s4}. But because these parameters have low values it is difficult to conclude. For instance, compared to the a priori values MY_c and MZ_c are good (taking into account that a variation of 10 $Kg.m$ on the value of a first moment component of the chassis is equivalent to a variation of 7 mm on the gravity center position since the chassis mass is about 1500 Kg). Parameters XY_c and YZ_c do not correspond to the a priori values but because of their low value w.r.t the diagonal elements XX_c, YY_c and ZZ_c they are physically hard to excite. Finally, concerning the parameters fs_1, fs_3, fs_4, they have no a priori values, but their values are negligible with respect to the offset forces of the suspension, thus these parameters can be eliminated.

TABLE II

RESULTS WITH 38 *dof* MODEL

parameters	units	a priori	estimated	$\sigma_{\hat{X}j}$	$\sigma_{\hat{X}j\%}$
M_c	Kg	1508.5	1496.6	2.2	0.1
MX_c	$m.Kg$	2421.1	2403.0	4.6	0.1
MY_c	$m.Kg$	0	8.7	1.6	19.1
MZ_c	$m.Kg$	-15.01	-12.2	3.7	30.5
XX_c	$Kg.m^2$	622.15	513.8	10.3	2.0
YY_c	$Kg.m^2$	5898	4856.7	132.3	2.7
ZZ_c	$Kg.m^2$	6199	6581.0	52.5	0.7
XZ_c	$Kg.m^2$	44.12	137.0	11.8	8.6
XY_c	$Kg.m^2$	76	-11.2	21.7	193.8
YZ_c	$Kg.m^2$	-13.00	-95.3	27.7	29.0
M_1	Kg	24	41.2	1.4	3.4
M_2	Kg	24	17.4	0.9	5.6
M_3	Kg	24	25.6	1.0	4.1
M_4	Kg	24	25.6	0.8	3.3
k_{arr}	N/m	19938	23639.0	450.5	1.9
k_{arf}	N/m	19033	21820.5	344.1	1.5
k_1	N/m	20600	26608.9	748.1	2.8
f_{s1}	N		9.1	3.3	36.4
h_1	$N/m/s$	3200	3528.4	96.7	2.7
off_1	N		12383.2	226.5	1.8
k_2	N/m	20600	26254.9	644.7	2.4
f_{s2}	N		35.8	2.2	6.3
h_2	$N/m/s$	3200	2981.1	70.2	2.3
off_2	N		12266.8	194.9	1.5
k_3	N/m	22000	26856.4	876.9	3.2
f_{s3}	N		2.1	3.0	144.2
h_3	$N/m/s$	3800	3832.5	106.2	2.7
off_3	N		10603.7	252.2	2.3
k_4	N/m	22000	31663.3	911.0	2.8
f_{s4}	N		5.0	3.2	64.1
h_4	$N/m/s$	3800	2599.8	107.0	4.1
off_4	N		12303.8	262.4	2.1
Cx			1.17158	0.00311	0.2

To validate the obtained values, the computed joint torques of the main joints, denoted by $\boldsymbol{Y}_j$, are compared with the reconstructed joint torques $\boldsymbol{W}_j \boldsymbol{X}$, where $\boldsymbol{X}$ is the vector of estimated parameters. Fig. 6 to 12 show cross validation results (the validation trajectory is a different sinusoidal steering trajectory than the one used for identification). Each figure shows the computed joint torque $\boldsymbol{Y}_j$, given by solid lines and the corresponding error $\boldsymbol{W}_j \boldsymbol{X}$- $\boldsymbol{Y}_j$, given with broken lines. For suspension, only one branch is given, the other branch results are similar. These curves show that the error signals are small w.r.t the total force or moment signals.

B. Identification with a 20 dof *model*

The 38 *dof* model used for the previous identification is quite complex. Indeed it takes into account half track width, wheelbase, toe, camber and kingpin angle variations. The same identification procedure is applied using the reduced 20 *dof* model shown in Fig.13, whose geometric parameters are given in Table III.

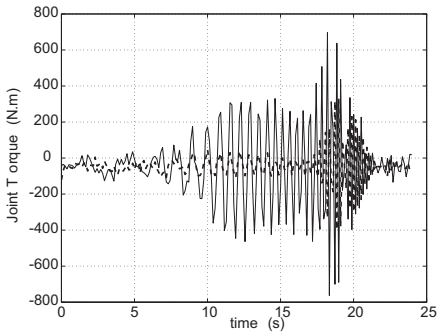

Fig. 6. Cross validation for the roll torque (Nm)

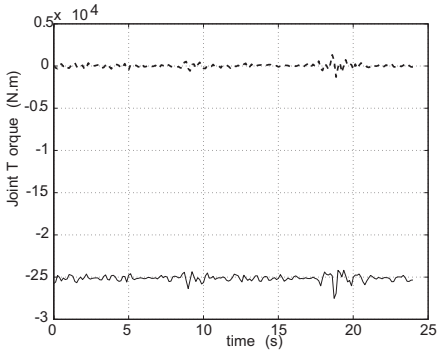

Fig. 7. Cross validation for the pitch torque (Nm)

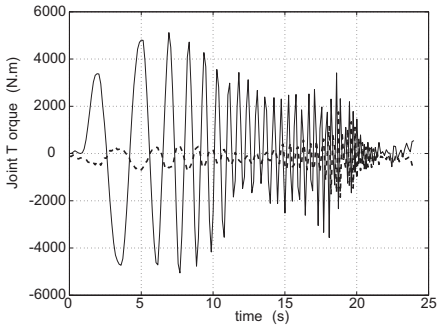

Fig. 8. Cross validation for the yaw torque (Nm)

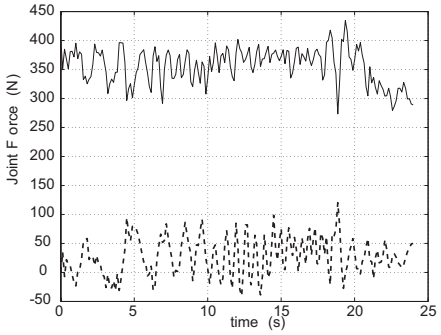

Fig. 9. Cross validation for the longitudinal force (N)

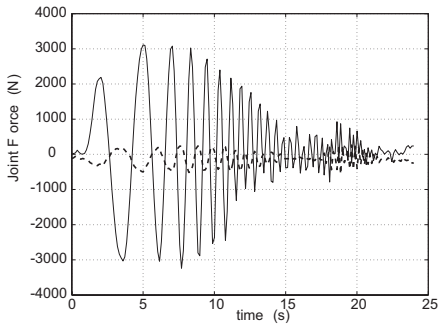

Fig. 10. Cross validation for the lateral force (N)

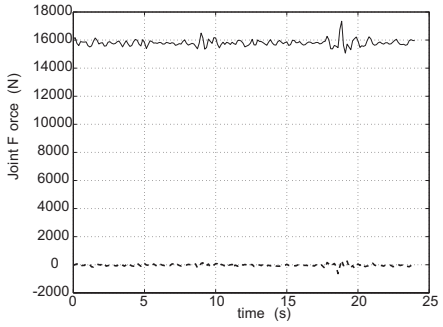

Fig. 11. Cross validation for the vertical force (N)

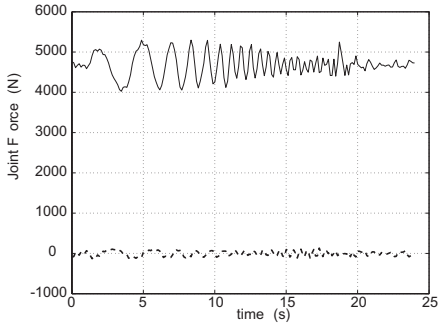

Fig. 12. Cross validation for the front left suspension force (N)

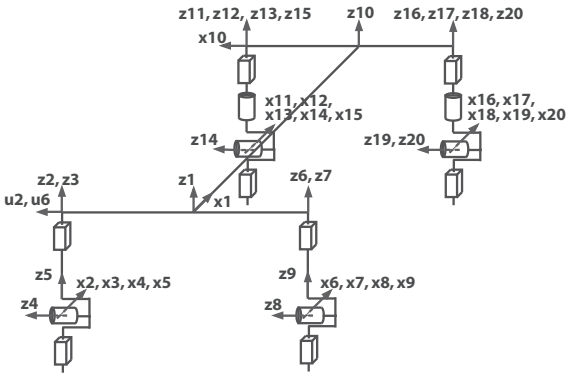

Fig. 13. The 20 *dof* model

TABLE III

THE GEOMETRIC PARAMETERS OF THE REDUCED 20 *dof* MODEL

j	$a(j)$	σ_j	γ_j	b_j	α_j	d_j	θ_j	r_j
1	0	2	0	0	0	0	0	0
2	1	1	$\pi/2$	0	0	l_3	$-\pi/2$	z_3
3	2	2	0	0	0	0	0	0
4	3	0	0	0	$-\pi/2$	0	θ_4	0
5	3	1	$\pi/2$	0	0	0	0	z_{t3}
6	1	1	$\pi/2$	0	0	$-l_4$	$-\pi/2$	z_4
7	6	2	0	0	0	0	0	0
8	7	0	0	0	$-\pi/2$	0	θ_8	0
9	7	1	0	0	0	0	0	z_{t4}
10	1	2	0	0	0	L	$\pi/2$	0
11	10	1	0	0	0	l_1	$-\pi/2$	z_1
12	11	0	0	0	0	0	β_1	0
13	12	2	0	0	0	0	0	0
14	13	0	0	0	$-\pi/2$	0	θ_{14}	0
15	13	1	0	0	0	0	0	z_{t1}
16	10	1	0	0	0	$-l_2$	$-\pi/2$	z_2
17	16	0	0	0	0	0	β_2	0
18	17	2	0	0	0	0	0	0
19	18	0	0	0	$-\pi/2$	0	θ_{19}	0
20	18	1	0	0	0	0	0	z_{t2}

Results of the identification on the 20 *dof* model are given in Table IV. They are very similar to those given in Table II obtained using the 38 *dof* model. Thus we conclude that the 20 *dof* model is sufficient for dynamic parameters identification.

VIII. CONCLUSION

This paper presents a new method to estimate the dynamic parameters of a car. The identification method is based on the use of robotics formalism in modelling tree structure multi-body systems. The model presented takes into account the most important *dof* of the chassis with respect to the ground and the wheels (38 *dof*). The use of the Euler variables for the chassis and the Lagrange variables for the other elements of the car is more convenient with respect to the car sensors and reduces model complexity.

With the use of the vehicle dynamic software ARHMM and real tests, a reduced model with 20 *dof* has been deduced for the identification of the chassis, the unsprung bodies and the suspension dynamic parameters. The sensors required are composed of an inertial unit, dynamometric wheels and suspension clearance measurements. The aerodynamic coefficient force along the longitudinal axis has also been identified.

Future work will be focused on the model extension to the interaction between the wheels and the ground. This model extension would enable us to extend the identification to the contact forces model with the goal of avoiding the use of dynamometric wheels.

REFERENCES

[1] Schmitt C.J. and al., "Identification of physical parameters of a passenger car," *ECC'99, Karlsruhe, Germany*, September 1999.

TABLE IV
RESULTS WITH 20 *dof* MODEL

parameters	estimated	$\sigma_{\hat{X}j}$	$\sigma_{\hat{X}j\%}$
M_c	1497.1	2.2	0.1
MX_c	2401.6	4.6	0.1
MY_c	8.2	1.6	20.0
MZ_c	−17.3	3.7	21.5
XX_c	518.7	10.2	1.9
YY_c	4858.9	132.4	2.7
ZZ_c	6636.7	61.8	0.9
XZ_c	145.7	11.8	8.1
XY_c	−12.6	21.7	171.4
YZ_c	−95.9	27.7	28.9
M_1	41.0	1.3	3.3
M_2	17.3	0.9	5.6
M_3	25.0	1.0	4.1
M_4	25.8	0.8	3.2
k_{adr}	23660.5	444.8	1.8
k_{adf}	21800.0	339.6	1.5
k_1	26608.6	738.4	2.7
fs_1	9.1	3.2	35.9
h_1	3526.8	95.5	2.7
off_1	12384.3	223.6	1.8
k_2	26280.3	636.4	2.4
fs_2	35.9	2.2	6.2
h_2	2980.7	69.3	2.3
off_2	12274.2	192.4	1.5
k_3	26815.8	865.7	3.2
fs_3	2.1	3.0	141.5
h_3	3832.4	104.8	2.7
off_3	10597.8	249.0	2.3
k_4	31628.4	899.5	2.8
fs_4	5.0	3.2	63.3
h_4	2597.5	105.7	4.0
off_4	12291.8	259.0	2.1
Cx	1.1	0.00363	0.31192

[2] Khalil W. and Kleinfinger J.-F., "Minimum operations and minimum pa-rameters of the dynamic model of tree structure robots," *IEEE J. of Robotics and Automation*, vol. RA-3(6), pp. 517–526, December 1987.

[3] Bodson P., *ARHMM V3.0 Guide utilisateur*, PSA - Peugeot Citroën, document interne edition, 2003.

[4] Kiencke U. and Nielsen L., *Automative Control Systems for Engine, Driveline and Vehicle*, 2000.

[5] Milliken W.F. and Milliken D.L., *Race car vehicle dynamics*, 1995.

[6] Pacejka H.B. and Besselink I.J.M., "Magic formula tyre model with transient properties," *Vehicle system dynamics*, , no. 27, pp. supplement, 1997.

[7] Pacejka H.B., *Tyre and Vehicle Dynamics*, Butterworth-Heinemann, 2002.

[8] Canudas de Wit C., Tsiotras P.and Velenis E., Basset M., and Gissinger G.L., "Dynamic friction models for road/tire longitudinal interaction," *Vehicle System Dynamics*, vol. 39, no. 3, pp. 189–226, 2003.

[9] Stéphant J., Charara A., and Meizel D., "Force model comparison on the wheel-ground contact for vehicle dynamics," in *IEEE Intelligent Vehicle Symposium, Versailles, France*, 2002.

[10] Khalil W. and Dombre E., *Modeling, identification and control of robots*, Hermès Penton, London-U.K, 2002.

[11] Guillo E.and Gautier M., "Dynamic modeling and identification of earthmoving engines without kinematic constraints," in *Proc. IEEE Int. Conf. on Robotics and Automation, San Francisco, CA, USA*, April 2000, pp. 2346–2351.

[12] Venture G., Khalil W., Gautier M., and Bodson P., "Dynamic modelling and identification of a car," in *15th IFAC world congress, Barcelona, Spain*, July 2002.

[13] Luh J.Y.S., Walker M.W., and Paul R.C.P, "On-line computational scheme for mechanical manipulators," *Trans. of ASME, J. of Dynamic Systems, Measurement, and Control*, vol. 102(2), pp. 69–76, 1980.

[14] Khalil w. and Bennis F., "Symbolic calculation of the base inertial parameters of closed-loop robots," *The Int. J. of Robotics Research*, vol. 14(2), pp. 112–128, April 1995.

[15] Gautier M., "Numerical calculation of the base inertial parameters," *J. of Robotic Systems*, vol. 8(4), pp. 485–506, August 1991.

[16] Gautier M., "Dynamic identification of robots with power model," in *Proc. Int. Conf. on Robotics and Automation, Albuquerque, USA*, 1997, pp. 1922–1927.

[17] Venture G., Khalil W., Gautier M., and Bodson P., "Parametric identification of a car dynamics," in *IFAC Symposium on System Identification, Rotterdam, Netherlands*, August 2003.

[18] Pressé C. and Gautier M., "New criteria of exciting trajectories for robot identification," in *Proc. IEEE Int. Conf. on Robotics and Automation, Atlanta*, 1993, pp. 907–912.

[19] Gautier M. and Khalil W., "Exciting trajectories for inertial parameters identification," *Int. J. of Robotics Research*, vol. 11(4), pp. 362–375, 1992.

[20] Gautier M., "Optimal motion planning for robot's inertial parameters identification," in *Proc. 31st IEEE Conf. on Decision and Control, Tucson*, 1992, vol. 1, pp. 70–73.

[21] Khalil W. and Creusot D., "Symoro+: a system for the symbolic modelling of robots," *Robotica*, vol. 15, pp. 153–161, 1997.

Gentiane Venture obtained an engineering degree and a Msc in automatic control and robotics from the Ecole Centrale de Nantes in 2000. In 2003, she completed her Ph.D thesis on the dynamic modelling and identification of car dynamics, supported by PSA and the IRCCyN, "Institut de Recherche en Communication et Cybernétique de Nantes" (France). She is now a research fellow of the the Univ. of Tokyo (Japan), supported by the Japan Society for Promotion of Science. Her research interests are modelling, identification and control of dynamic systems.

Pierre-Jean Ripert obtained an engineering degree and Msc in automatic control and robotics from the Ecole des Mines de Nantes and the Ecole Centrale de Nantes respectively in 2003. He is now Ph.D student supported by PSA and the IRCCyN, "Institut de Recherche en Communication et Cybernétique de Nantes" (France) on tire identification both from test benches and car measurements. His research interests are the modelling, identification, interval analysis and robust control.

Wisama Khalil obtained a Ph.D and "Doctorat d'Etat" degree in Robotics and Control Engineering from Montpellier (France) in 1976 and 1978 respectively. Since 1983 he has been professor at the Automatic Control and Robotics department of the Ecole Centrale de Nantes (France). He is carrying out his research within the robotics team of the IRCCyN, "Institut de Recherche en Communication et Cybernétique de Nantes". His research topics include modelling, control and identification of robots.

Maxime Gautier obtained a "Doctorat d'Etat" degree in Robotics and Control Engineering from Nantes (France) in 1990. Since 1991 he has been professor in Automatic Control at the University of Nantes. He is carrying out his research within the robotics team of the IRCCyN, "Institut de Recherche en Communication et Cybernétique de Nantes". His research topics include modelling, identification and control of robots.

Philippe Bodson obtained an electro-mechanical engineer diploma at Liege University in 1991. He worked until 1997 in the SERA-CD in the field of the Vehicle Dynamics. He now works for the French car manufacturer PSA Peugeot Citroën as manager of the vehicle dynamics modelling team, with a special emphasis on correlation between simulations and tests on track.